Supplementary Information

Organic Photocatalysts Enable Efficient Hydrogen Production via Förster Resonance Energy Transfer

Mengmeng Han*[a], Wei Li[b], Lingpan Lu[a], Rui Li[a], Xin Ma[a], Meng Chen[c]*, Jingshuai Zhu*[d], Zhenqiang Yang[a]

[a.]Institute of Chemistry, Henan Academy of Sciences, Zhengzhou, Henan, 450002, China

[b.]Institute of Laser Manufacturing, Henan Academy of Sciences, Zhengzhou 450046, China

[c.]Zhengzhou University, Zhengzhou 450001, China.

[d.]School of Fashion and Textiles, The Hong Kong Polytechnic University, Kowloon, 999077, Hong Kong.

Experimental section

Chemicals and materials

Chloroform was purchased from Xilong Scientific Co. Ltd. D18 and Compound 1 were purchased from Hyper Inc. IT-M and 2F-IC were purchased from SunaTech Inc. QX-1 was synthesized according to procedures reported in the literature.[S1]

Synthesis

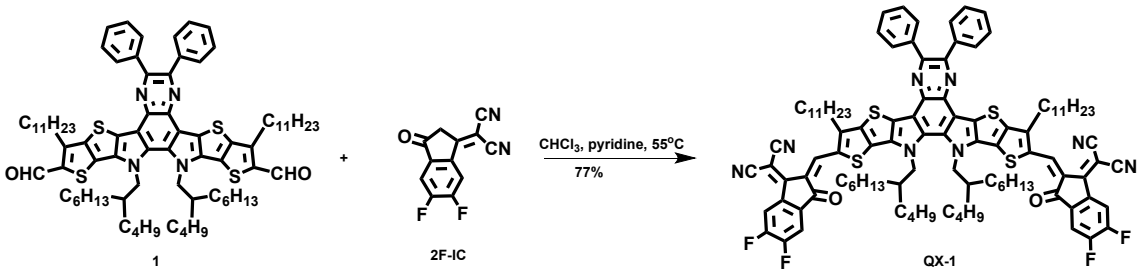

Scheme S1. Synthetic route to QX-1.

QX-1. compound 1 (105 mg, 0.1 mmol), 2F-IC (115 mg, 0.5 mmol), pyridine (0.5 ml), and chloroform (20 ml) were added to a three-necked round-bottom flask. The mixture was then deoxygenated with nitrogen for 20 min and stirred for 15 h. After cooling to room temperature, the mixture was poured into methanol (150 ml) and filtered. The residue was purified by silica gel column chromatography using petroleum ether: dichloromethane (1:1.5) as the eluent, yielding a black solid (113 mg, 77%). ^{1}H NMR (400 MHz, $CDCl_3$): δ 9.19 (s, 1H), 8.59 (dd, J = 9.9, 6.4 Hz, 1H), 7.81 (dd, J = 6.6, 2.9 Hz, 2H), 7.72 (t, J = 7.5 Hz, 1H), 7.51 – 7.45 (m, 3H), 4.83 (d, J = 8.3 Hz, 2H), 3.29 (t, J = 7.9 Hz, 2H), 2.22 (s, 1H), 1.89 (p, J = 7.9 Hz, 2H), 1.53 (q, J = 7.7 Hz, 1H), 1.29 (dd, J = 14.2, 4.3 Hz, 13H), 1.18 – 0.83 (m, 7H), 0.77 – 0.63 (m, 6H).

^{13}C NMR (100 MHz, $CDCl_3$): δ 151.01, 139.36, 131.02, 130.48 – 130.19, 128.83, 128.38, 55.55, 39.13, 31.93, 31.63, 31.50, 29.77, 29.71, 29.64, 29.77 – 29.29 , 29.37, 27.95, 25.36, 22.90, 22.71, 22.50, 14.14, 14.07, 13.85.

MS (MALDI-TOF): m/z 1708.9 (M+).

Anal. Calcd for $C_{104}H_{112}F_4N_8O_2S_4$: C, 73.04; H, 6.60; N, 6.55; Found: C, 73.08; H, 6.47; N, 6.62.

Characterization and molecular simulations

Nuclear magnetic resonance (NMR) spectra were obtained with a Bruker 400 MHz spectrometer. Mass spectra measurements were carried out on a Bruker Daltonics Biflex III MALDI-TOF Analyzer in the MALDI mode. Elemental analyses were conducted using a FLASH EA1112 elemental analyzer. Fourier transform infrared spectroscopy (FT-IR) was performed using a Thermo Fisher Nicolet Is5 with a thin KBr pellet. Differential scanning calorimetric (DSC) and thermogravimetric analyses (TGA) were performed on a NETZSCH STA-2500 instrument with a heating rate of 10 K min^{-1} under a nitrogen atmosphere. Ultraviolet and visible (UV-vis) absorption spectra were recorded using a SHIMADZU UV 3600I plus spectrophotometer. Photoluminescence (PL) spectra were gathered using an EDINBURGH FLS-1000 fluorescence spectrometer. The morphology of the Circular cellulose substrate was observed using Scanning electron microscopy (SEM, thermo scientific Apreo 2C).

DFT calculation:

All calculations were carried out with the Gaussian 09 software.[S2] The geometry and the hydrogen evolution reaction (HER) for D18, IT-M, and QX-1 were optimized using the B3LYP level of theory in conjunction with the 6-31G (d) basis set[S3, S4] with Grimme's DFT-D3(BJ) empirical dispersion correction[S5]. All geometries were fully optimized and the vibrational frequencies were performed at the same level to confirm that all geometries locate at the minimal, and gained Gibbs free energy at 298.15 K and 1 atm. It should be noted that the Gibbs free energies of HER intermediates in the reaction pathways were calculated from the computational hydrogen electrode (CHE)

model according to the study of Nørskov et al.[S6,S7] The reversible hydrogen electrode (RHE) was regarded as a reference, then the chemical potential of the H^+/e^- pair is equal to half of the gas-phase H_2 at 0 V potential and 1 atm.[S8,S9] The electrostatic potential (ESP) for studied molecules were calculated and plotted by GaussView 6.0.16.

Hydrogen evolution

The solutions (0.5 mg ml^{-1}) of D18:QX-1 (mass ratio is 1:2), D18:IT-M:QX-1 (mass ratio is 1:0.5:1.5) were prepared in chloroform. The solutions were heated at 50 ℃ for 2 h and then stirred at room temperature overnight, circular cellulose substrate were immersed in chloroform solutions. Then natural drying in the fume hood removes the chloroform solvent. The photochemical reaction system (PerfectLight, labsolar 6A) is applied to screen the optimal hydrogen evolution conditions and recycling stability among D18:QX-1 and D18:IT-M:QX-1. The photocatalytic reaction platform formed from various conditions are respectively added into each off-line reactor (photocatalytic reaction platform area, 16 cm^2, penetration depth of light, 2 cm) with 0.2 M L-ascorbic acid (AA) in aqueous solution, and then the reactors are purged with nitrogen several times to remove oxygen, and the pressure is set to 8 KPa. Potassium hexachloroplatinate precursor solution (K_2PtCl_6, 1 mg ml^{-1}) is used for photo-depositing cocatalyst Pt (20 wt% Pt, at room temperature). The hydrogen evolution is evaluated by an online gas chromatograph. The optimal hydrogen evolution condition is used to obtain the hydrogen evolution rate (HER) under simulated solar light. For hydrogen production from seawater, 0.2M AA is also added to seawater, and then the reactors are purged with nitrogen to remove oxygen. Potassium hexachloroplatinate precursor solution (K_2PtCl_6, 1 mg ml^{-1}) is used for photo-depositing cocatalyst Pt (20 wt%). For the recycling experiment of hydrogen evolution of D18:IT-M:QX-1 photocatalytic reaction

platform (20 wt% Pt, at room temperature), the equivalent amount of AA is added after the end of every cycle (4 h) according to the consumption of AA. The photocatalytic reaction platform in aqueous solution with 0.2 M AA and a certain amount of K_2PtCl_6 aqueous solution (1 mg ml^{-1}, 20 wt% Pt) is added into the recirculating batch reactor (photocatalytic reaction platform area, 16 cm^2, penetration depth of light, 2 cm). The hydrogen evolution is evaluated by an all-glass automatic online trace gas analysis system (PerfectLight, Labsolar-6A) with an online gas chromatograph, and the photocatalytic reaction platform is illuminated with a 300 W Xe lamp equipped with a mirror module (320-1100 nm). The illumination intensity in this study is 198 mW cm^{-2} in all circumstances.

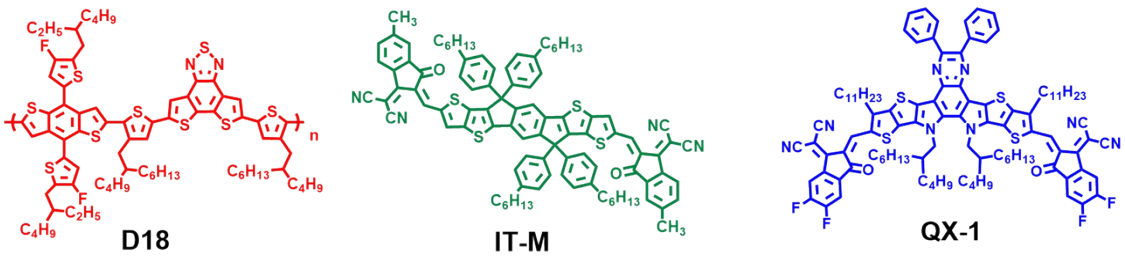

Fig. S1 Molecular structure of D18, IT-M, and QX-1.

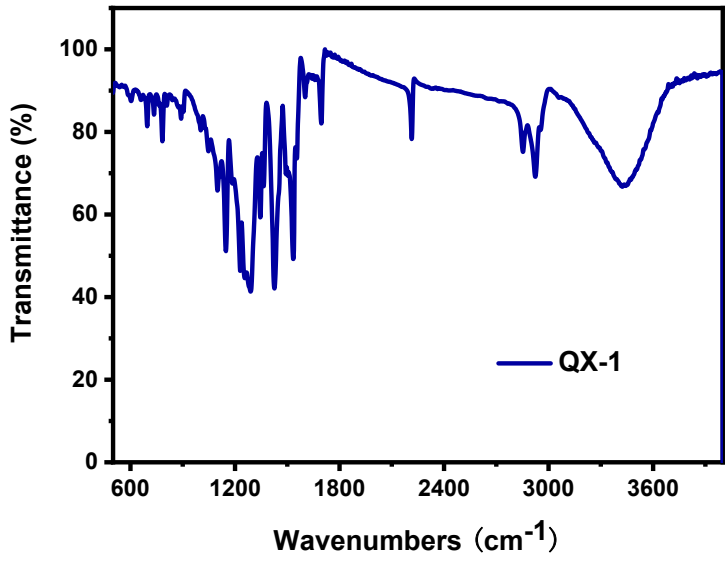

Fig. S2 FT-IR spectra of QX-1.

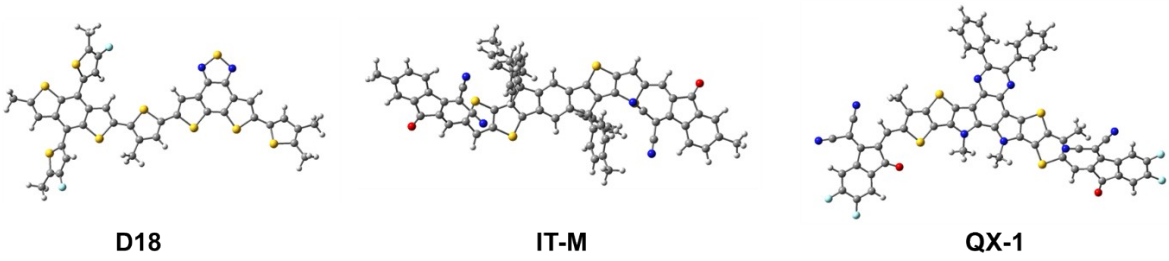

Fig. S3 Optimized ground-state geometry for D18, IT-M, and QX-1.

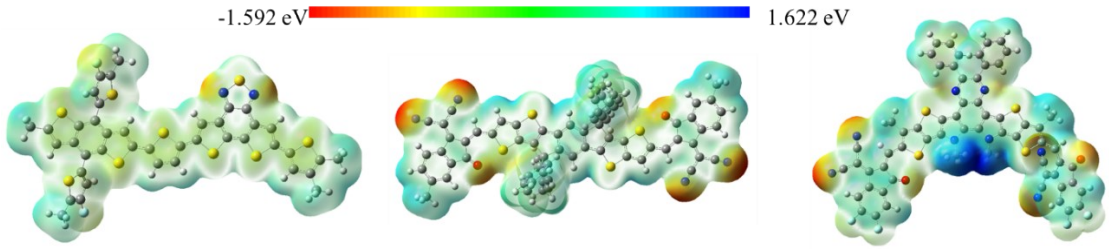

Fig. S4 The ESP plots for D18, IT-M, and QX-1, where the molecular surface is defined as the isovalue of electron density equaling to 0.001 a.u. proposed by Bader et al.[11]

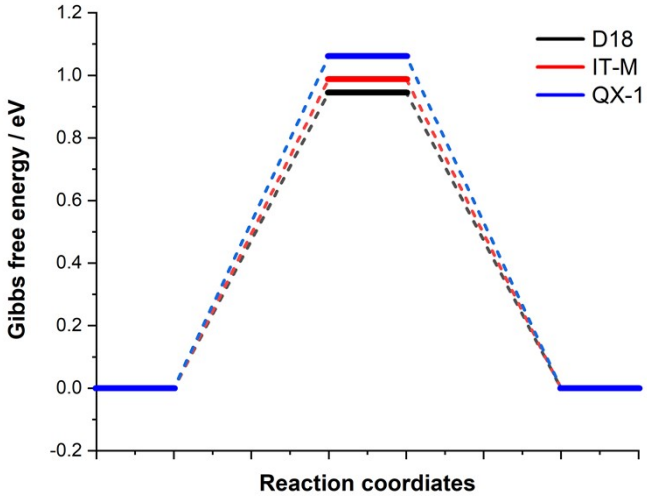

Fig. S5 The Gibbs free energy profile for HER.

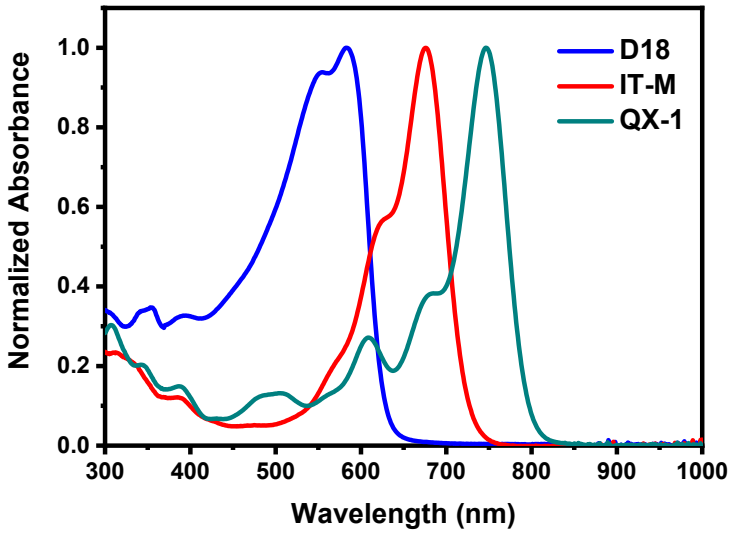

Fig. S6 UV-Vis absorption spectra of D18, IT-M, and QX-1 in chloroform solution (10^{-6} M).

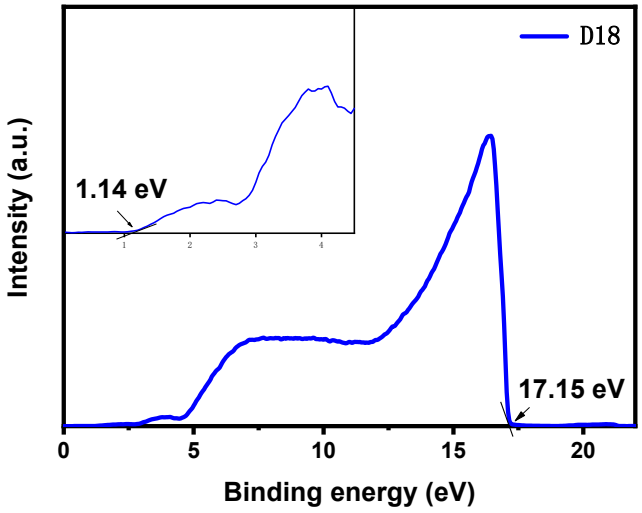

Fig. S7 UPS data of the D18 film.

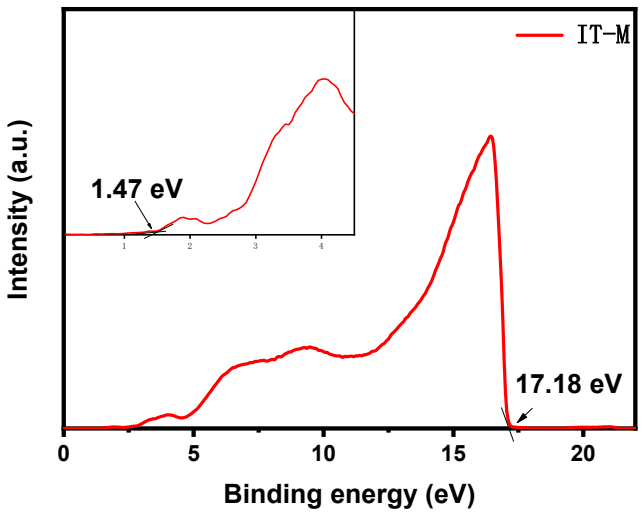

Fig. S8 UPS data of the IT-M film.

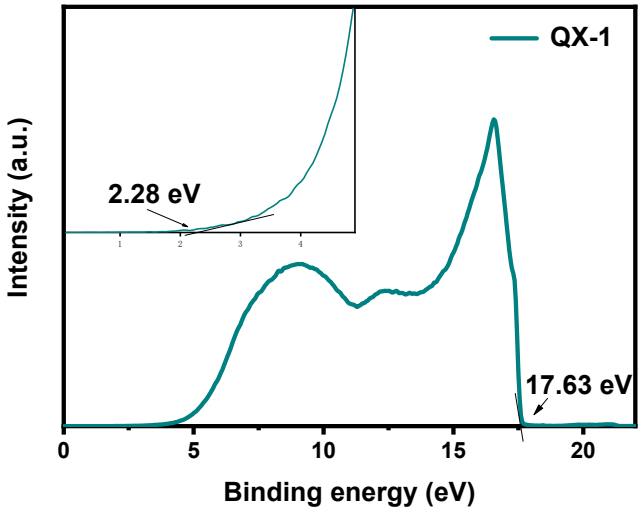

Fig. S9 UPS data of the QX-1 film.

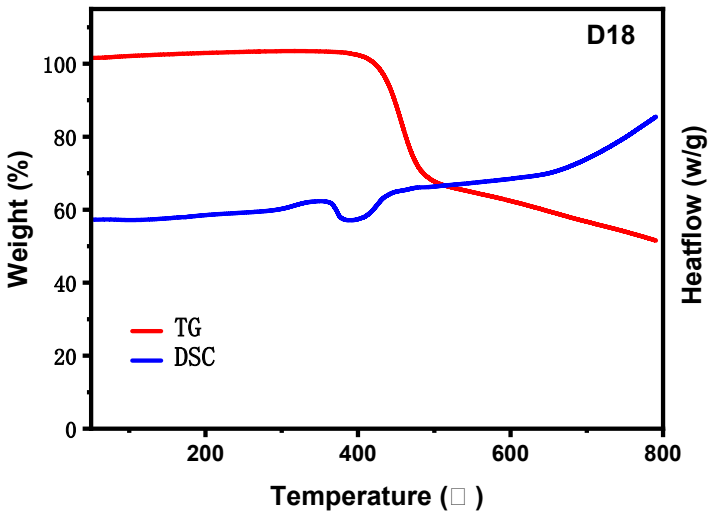

Fig. S10 TG-DSC data of the D18 solid.

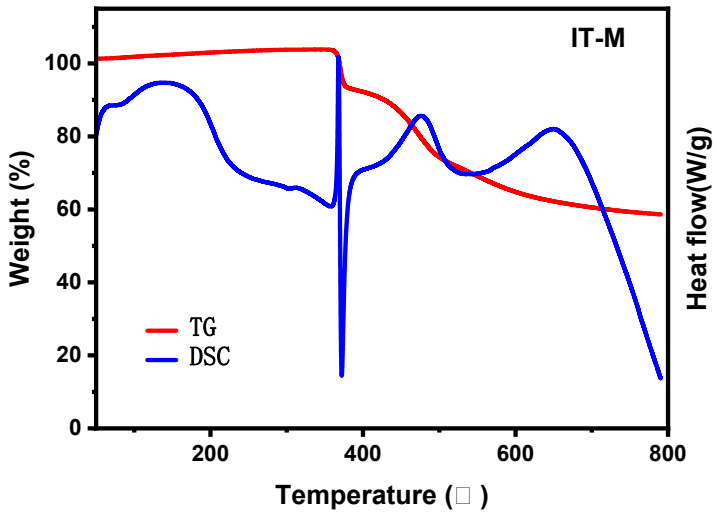

Fig. S11 TG-DSC data of the IT-M solid.

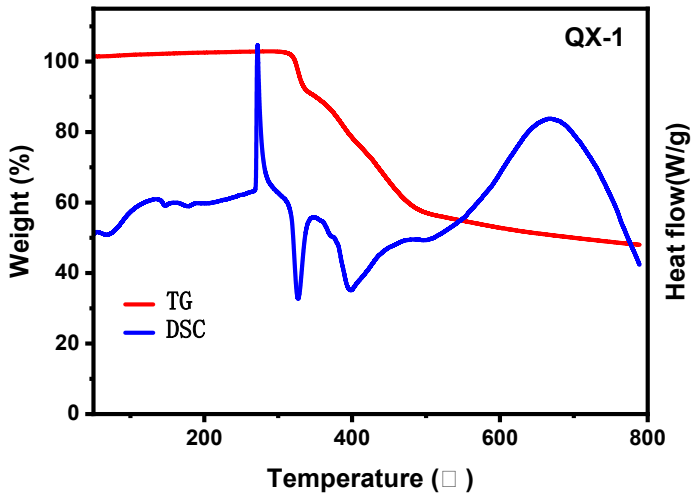

Fig. S12 TG-DSC data of the IT-M solid.

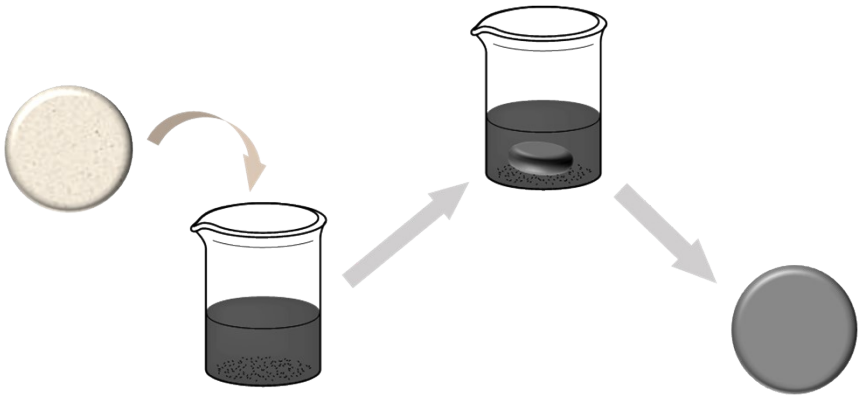

Fig. S13 Schematic of process for the photocatalytic reaction platform by soak method.

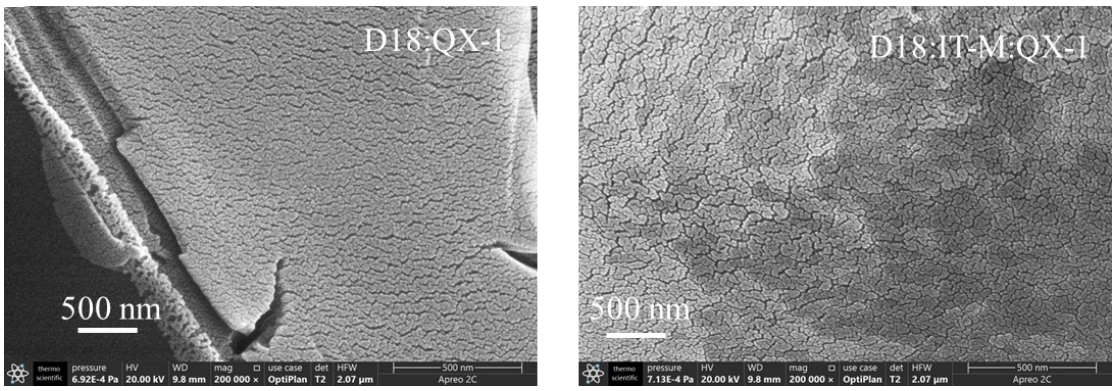

Fig. S14 SEM images of D18:IT-M:QX-1 and D18:QX-1-cellulose under 200 000X.

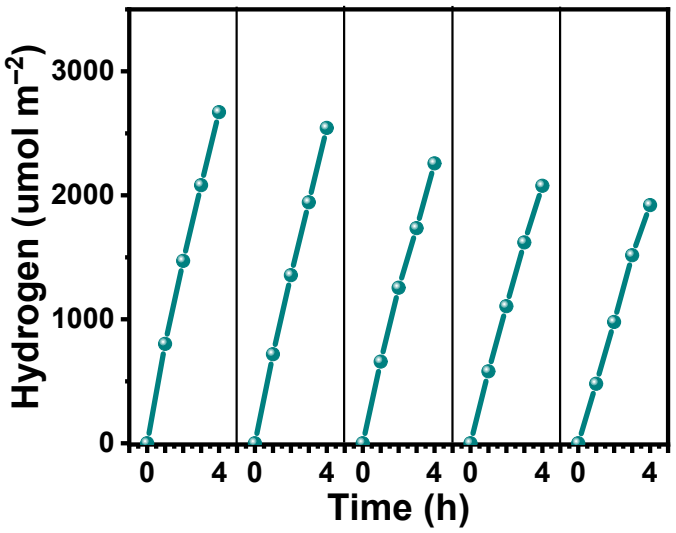

Fig. S15 The stable cyclic photocatalytic HER rate of D18:IT-M:QX-1.

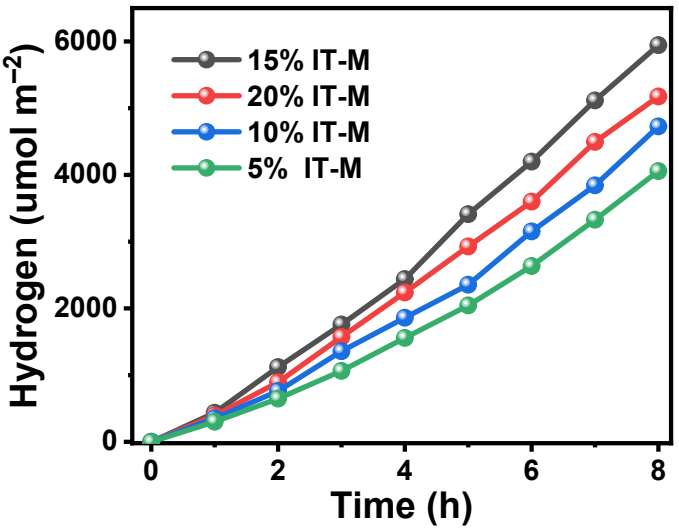

Fig. S16 Optimization of IT-M content in D18:IT-M:QX-1 reaction platform hydrogen evolution experiments.

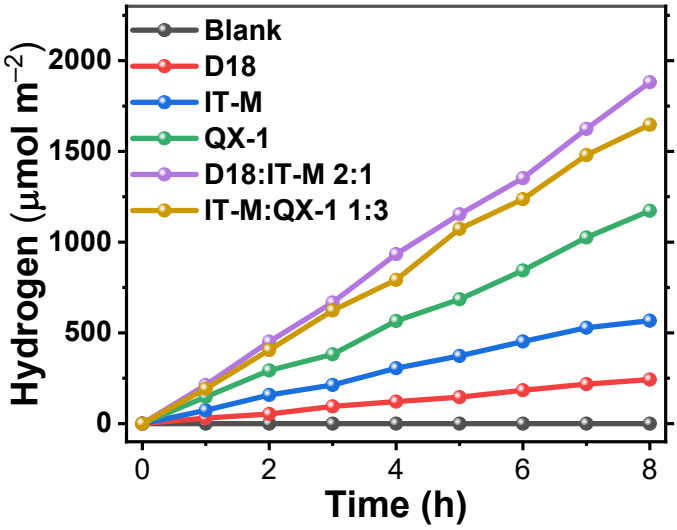

Fig. S17 The hydrogen evolution experiments of blank cellulose substrate, single-component, two-component reaction platform under light intensity of 198 mW cm^{-2} (20% Pt loadings).

Table S1 The summary of the photocatalytic performances of photocatalysts for hydrogen evolution from water splitting.

	Co-catalyst	Sacrificial agent	Light Source	HER rate	Ref
D18:IT-M:QX-1	Pt	Ascorbic Acid	AM 1.5G	7430 μmol h^{-1} m^{-2}	This work
PM6:Y6 NPs	Pt	Ascorbic Acid	AM 1.5G	43.9 mmol h^{-1} m^{-2}	*Nat. Energy* **7**, 340–351 (2022).
PM6:PCBM NPs	Pt	Ascorbic Acid	AM 1.5G	73.7 mmol h^{-1} m^{-2}	*Nat. Energy* **7**, 340–351 (2022).
PM6:TPP NPs	Pt	Ascorbic Acid	AM1.5 G	72.75 mmol h^{-1} m^{-2}	*Angew. Chem. Int. Ed.* **2022**, *61*, e202114234
PTB7-Th:EH-IDTBR NPs	Pt	Ascorbic Acid	AM1.5 G	69.75 mmol h^{-1} m^{-2}	*Nat. Mater.* **2020**, *19*, 559–565;

References

S1. Shi Y, Chang Y, Lu K, et al, Small reorganization energy acceptors enable low energy losses in non-fullerene organic solar cells, *Nat Commun*, 2022, **13**, 3256.

S2. Frisch M, Trucks G, Schlegel H, et al, Gaussian 09, revision D. 01. In Gaussian, Inc., Wallingford CT: 2009.

S3. Becke A, Density-functional thermochemistry. III. The role of exact exchange. *J. Chem. Phys*, 1993, **98**, 5648–5652.

S4. Petersson G; Al-Laham M. A complete basis set model chemistry. I. The total energies of closed-shell atoms and hydrides of the first-row elements. *J. Chem. Phys*, 1988, **89**, 2193–2218.

S5. Grimme, S.; Ehrlich, S.; Goerigk, L. Effect of the damping function in dispersion corrected density functional theory. *J. Comput. Chem.* 2011, **32**, 1456-1465.

S6. Peterson, A. A.; Abild-Pedersen, F.; Studt, F.; Rossmeisl, J., How copper catalyzes the electroreduction of carbon dioxide into hydrocarbon fuels. *Energy Environ. Sci.* 2010, **3**, 1311-1315.

S7. Nørskov, J. K.; Bligaard, T.; Logadottir, A.; Kitchin, R.; Chen, G.; Pandelov, S.; Stimming, U., Trends in the Exchange Current for Hydrogen Evolution. *J. Electrochem. Soc.* 2005, **152**, J23-J26.

S8. Peterson, A. A.; Nørskov, J. K., Activity Descriptors for CO_2 Electroreduction to Methane on Transition-Metal Catalysts. *J. Phys. Chem. Lett.* 2012, **3**, 251-258.

S9. Nørskov, J. K.; Rossmeisl, J.; Logadottir, A.; Lindqvist, L., Origin of the Overpotential for Oxygen Reduction at a Fuel-Cell Cathode. *J. Phys. Chem. B* 2004, **108**, 17886-17892.

S10. Bader, R. F. W.; Carroll, M. T.; Cheeseman, J. R.; Chang, C., Properties of atoms in molecules: atomic volumes. *J. Am. Chem. Soc.* 1987, **109**, 7968-7979.